Oil & Gas Science and Technology – Rev. IFP, Vol. 58 (2003), No. 1, pp. 151-162

Modeling of Diesel Particulate Filter Regeneration, with the Effect of Fuel-Borne Catalyst on Pressure Losses and Soot Oxidation Kinetics

C.N. Millet[1*], P. Ménégazzi[1], B. Martin[1], H. Colas[2]

1 Institut français du pétrole, division Techniques d'applications énergétiques, CEDI « René Navarre », BP3, 69390 Vernaison - France
2 PSA Peugeot-Citroën, 18, rue des Fauvelles, 92256 La Garenne-Colombes Cedex - France
c-noelle.millet@ifp.fr - pascal.menegazzi@ifp.fr - brigitte.martin@ifp.fr - herve.colas@mpsa.com

*Corresponding author

Résumé — Modélisation de la régénération du filtre à particules Diesel : effet de l'additif — Étant donné les phénomènes complexes qui entrent en jeu dans la régénération du filtre à particules Diesel (DPF en anglais), la modélisation constitue une aide précieuse pour en optimiser la mise en place et le contrôle. En particulier, l'action de l'additif doit être prise en compte, en raison de son effet prédominant sur l'initiation de la combustion des suies et la propagation de la régénération. Cet article décrit le modèle 1D développé à l'*IFP* en partenariat avec *PSA*, qui permet de simuler le chauffage, l'allumage, et l'oxydation des suies à travers le filtre à effet *wall-flow*. Le but est de prédire la régénération d'un canal du filtre, le débit, la température et la composition en oxygène des gaz d'échappement, ainsi que la façon dont le filtre a été préalablement chargé. Le mécanisme réactionnel et les lois cinétiques ont été étudiés expérimentalement et tiennent compte de l'action de l'additif. Des essais sur banc moteur ont été réalisés pour mettre en évidence les effets de l'additif, ainsi que la sensibilité de la régénération aux principaux paramètres (caractéristiques des gaz d'échappement et de la suie piégée dans le filtre). Il a été trouvé, entre autres, que la suie additivée tend à être balayée vers le fond des canaux, ce qui modifie l'évolution de la régénération, et que la température d'initiation de combustion varie avec le type de suie.

Les résultats expérimentaux forment une base de données qui nous a permis de valider le modèle pour plusieurs configurations. Il apparaît que les simulations sont en bon accord avec les résultats expérimentaux. Le modèle est donc un outil fiable pour prédire l'évolution de la régénération du filtre à particules, avec et sans additif.

Abstract* — *Modeling of Diesel Particulate Filter Regeneration: Effect of Fuel-Borne Catalyst — *Modeling is a valuable help to optimize the setting and control of Diesel particulate filter (DPF) regeneration, given the complex phenomena involved. Among those, the fuel-borne catalyst action must be taken into account, because of its prevailing effect on the soot ignition and the regeneration propagation. This paper describes how a 1D model was developed at* IFP, *in a collaboration with* PSA, *which simulates the soot heating, ignition and oxidation along the wall-flow filter. The aim is to predict the regeneration of one filter channel, knowing the exhaust gases flow, temperature and oxygen content, and the way the filter was loaded with soot. The reaction mechanism and kinetics were experimentally studied and involve the additive action. Engine bench tests were conducted to highlight the effects of additive content, as well as the regeneration sensitivity to its main parameters (exhaust gases and soot features). Among others, it was found that additivated soot tend to pack down in the bottom of the inlet*

channels, thus modifying the regeneration progress, and that ignition temperature varies with the soot type.

The experimental results obtained yielded a data base, which allowed us to validate the model for various configurations. The simulations appeared to be in good agreement with experimental results. The model is thus a reliable tool to predict the progress of the filter regeneration, with and without fuel-borne catalyst.

NOTATIONS

- a Parameter in square channel pressure drop correlation, 28.45
- D Channel width (m)
- c_p Specific heat capacity ()
- E_a Activation energy(J/mol)
- h Heat convection coefficient at wall (J/m^2/s/K)
- K Pre-exponential factor
- k Permeability (m^2)
- L DPF length (m)
- m Carbon mass (kg)
- P Pressure (Pa)
- R Perfect gas constant (J/mol/K)
- r Perfect gas constant for air (287 J/kg/K)
- T Temperature (K)
- t Time (s)
- v Gas velocity (m/s)
- x Distance through porous medium (m)
- Y Oxygen mass fraction
- w Thickness of the particulate deposit layer (m)
- w_s Thickness of wall of monolith channel (m)
- z Axial distance (m).

Greek letters

- α Order of reaction of oxygen
- β Order of reaction of carbon
- ε Fraction of oxidized metallic sites
- ΔH Specific heat of combustion (J/mol C)
- Φ_w Linear gas mass flow through particulate deposit layer (kg/m/s)
- λ Conductivity (W/m/K)
- μ Viscosity (kg/m/s)
- ρ Density (kg/m^3)
- δ Fuel-borne catalyst content
- ζ Oxidized carbon fraction.

Indexes

- 0 Initial value
- 1 Inlet channel
- 2 Outlet channel
- g Gas
- p Particulate
- s Substrate (SiC)
- w Particulate deposit layer.

INTRODUCTION

The Diesel particulate filter (DPF) is now being used on passenger cars, city buses, as well as some lift-forked trucks and fixed installations, as it is the most efficient device for reducing soot emissions. The development of such a technology requires the implementation of advanced engine management strategies aimed at periodically regenerating the trap. Under the conditions usually met in the exhaust gases flowing through the DPF, the soot ignition temperature exceeds 550°C. Such high exhaust temperatures are only observed during high load operation, which is usually not attained in city driving conditions. The use of a fuel-borne catalyst, also called additive, is required to decrease the soot ignition temperature down to 450°C and to allow DPF regeneration thanks to adapted engine tuning [1]. It is therefore a dominant parameter in the development of regeneration strategies.

Modeling is very helpful to understand the complex physical phenomena occurring during the regeneration, especially when an additive is used, since it induces a more violent regeneration, sometimes accompanied by a sharp temperature increase, which may damage the trap. A number of papers has already been published on the subject, for several kinds of additives [2, 3]. Some of the models only simulate the thermal and chemical processes across the particulate deposit layer, assuming that the gas flow rate is large enough to allow the temperature gradients along the lengths of the channel to be neglected. But circumstances quite often occur in which these axial variations cannot be neglected. A complete model must therefore describe both the gas flow characteristics (local variations along the channels, global back-pressure), the competition between the gas and trap temperatures, and the heating due to the soot oxidation [4, 5].

The purpose of this research is to formulate such a 1D general model, to solve the resulting system of differential equations, while taking into account the specific action of the fuel-borne catalyst. It includes pressure variations in the channels, conductive and convective transport of heat and

oxygen between the channel gas and the walls, as well as the effect of reaction-generated temperature increases on the particle depletion rate.

The soot was obtained on an engine test bench. The kinetics were determined by running experiments on a fixed bed reactor. DPF regeneration tests were run on the engine test bench to validate our model in realistic conditions. Several kinds of soot, different additive contents were studied, both experimentally and numerically. The influence of the exhaust gases (mass flow, oxygen content) was also investigated. The experimental setup and results are first presented, then the model and its validation are described.

1 EXPERIMENTAL SETUP

Our engine test bench is equipped with a *PSA* DW10 ATED engine. The exhaust line includes an oxidation catalyst and a wall-flow particulate trap.

We used a 5.66" × 6" "wall-flow" monolith filter, made of silicon carbide (SiC) by extrusion. Plugging adjacent channels alternately at opposite ends forces the exhaust stream through the porous ceramic walls, to give the flow pattern indicated in Figure 1. Solid particulate in the exhaust stream are trapped on the upstream sides of the channel walls typically with greater than 90% efficiency. The porosity of the walls is chosen so that particles in the exhaust quickly bridge over or plug the pores at the upstream lateral surfaces of the long channels. As more particle-laden gas flows through the monolith, the previously deposited particle layer then filters the particles in the subsequently filtered gas.

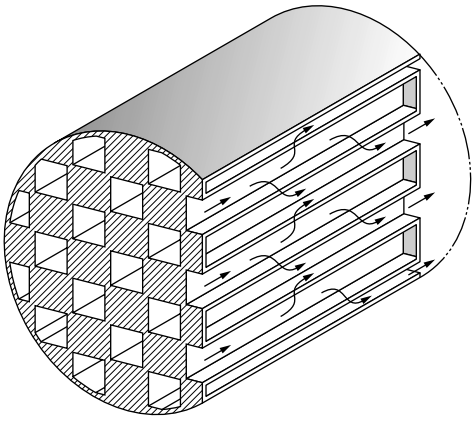

Figure 1

Schematic view of the DPF (Bissett and Shadman [6]*).

* Reproduced with permission of the *American Institute of Chemical Engineers*, Copyright © 1985 *AIChE*. All rights reserved.

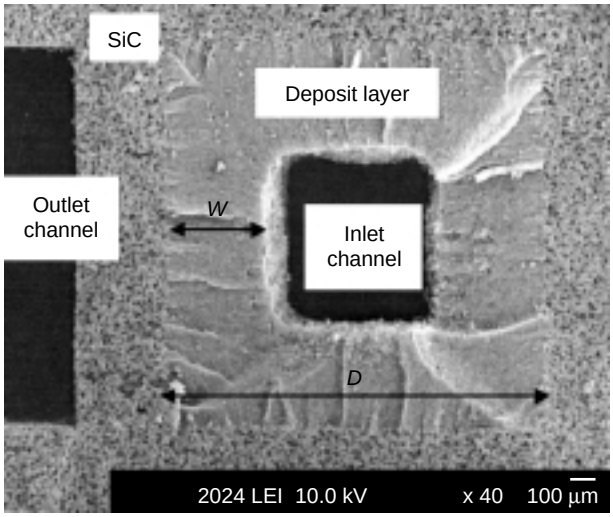

Figure 2

Scanning electron micrograph of the fractured edge of a loaded DPF.

The Figure 2 is a micrograph of a section of loaded monolith and shows how this process results in the formation of a cake of deposit on the upstream side of the channel walls with little penetration into the interior pores of the monolith. Downstream of the trap, the gases have an ultra low level of carbonaceous particles. As the thickness of the deposit increases, it provides an increasing resistance to the gas flow, necessitating the regeneration of the filter in order to avoid extra fuel consumption.

As shown on Figure 3, the experimental setup is different depending on whether we are loading or regenerating the trap. For regeneration tests, two additional devices are inserted between the engine and the after-treatment system: a heater, which can heat the exhaust gases up to 580°C, and another particulate trap which is only used for filtering the particle-laden gases and keeping the heater clean. The oxidation catalyst and the DPF are put into a lagging to reduce heat losses.

Two engine points were investigated to load the DPF: a high load point characteristic of EUDC (extra urban driving cycle) conditions (2580 tr/min, 97 Nm), and a load point characteristic of ECE (urban driving cycle) conditions (2030 tr/min, 21.4 Nm). The fuel was additivated with 2 different additive contents: 25 and 50 ppm. Each DPF was loaded with about 10 g/l of soot, and weighed before being set up for the regeneration test. The pressure drop and the downstream gas composition (O_2, CO, CO_2, HC, NO_x), were continuously measured. Nine thermocouples, 1 mm in diameter, were distributed in the DPF, as shown on Figure 4, to monitor the regeneration progress.

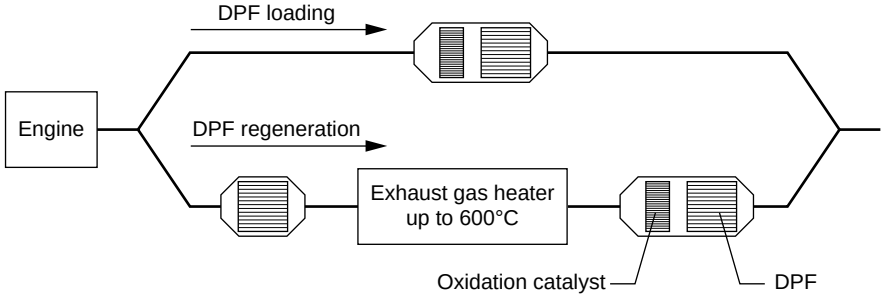

Figure 3

Experimental set up.

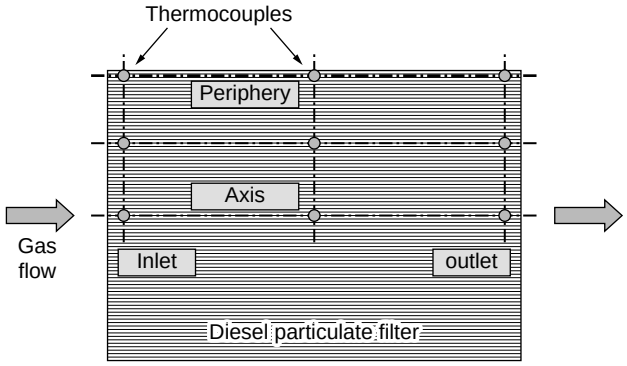

Figure 4

Thermocouples locations in DPF.

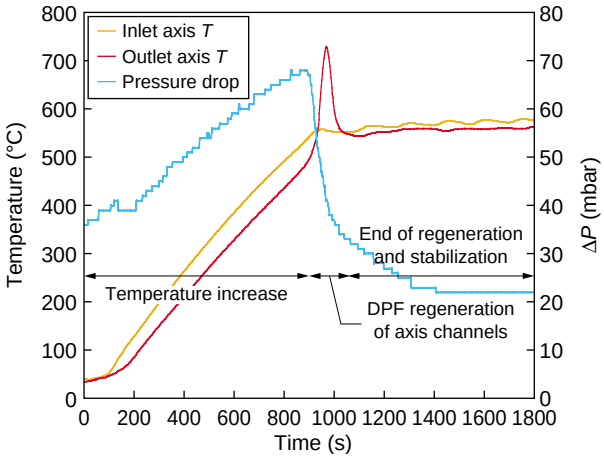

Figure 5

A typical regeneration test (1 mbar = 100 Pa).

Regenerations were run with four different operating conditions, allowing us to study the effect of the oxygen content (10 and 15%) and the gas flow rate (about 80 and 145 kg/h). Some other properties of the exhaust gases did change as well when varying operating conditions, such as the HC and NO_x contents, but we assumed that the oxygen and flow rate effects were dominant.

2 EXPERIMENTAL RESULTS

A typical example of a DPF regeneration on our engine test bench is shown on Figure 5, where the time evolution of the temperature (channel inlet and outlet) and the pressure drop are given. Three steps stand out:

– The DPF temperature and the pressure drop first increase, as the exhaust gases are heated by the heater.
– The reaction starts to become significant, and the filter temperature exceeds the inlet temperature. The particulate deposit layer starts to burn around 470°C, reaching a peak temperature that sometimes exceeds 1000°C, and high thermal gradients that may be detrimental to the filter durability. The pressure drop decreases rapidly as the soot oxidizes. The highest heat release always occurs nearby the outlet of the trap, where the major part of the intake gases has already flowed through the deposit layer, and cannot play its temperature regulator function anymore.
– Finally, the regeneration ends, and the backpressure stops dropping.

2.1 Exhaust Gases Characteristics

As shown on Figure 6, the exhaust gases flow rate has a direct effect on soot oxidation: the higher the flow rate, the

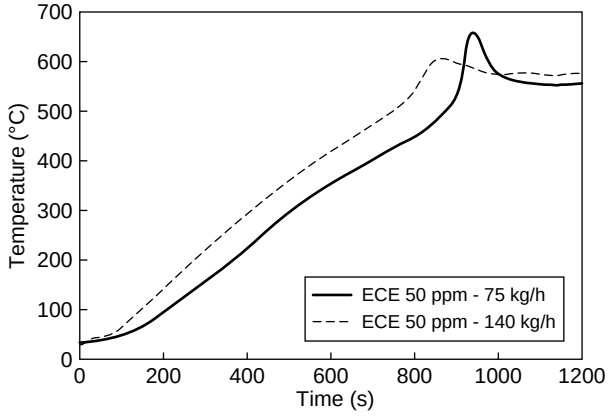

Figure 6

Exhaust gases flow rate effect.

lower the peak temperature. But the DPF is also heated faster, with the result that the total regeneration does not take longer. The flow rate has no effect on the soot ignition temperature.

The regeneration behavior also depends on the exhaust gases oxygen content. But in our investigations, both chosen concentrations (10 and 15%) appeared to be high enough to ensure a fast oxidation, and we did not see any difference in our experimental results.

2.2 Soot Type

We consider that the soot ignition temperature is reached when the time derivative of the channel outlet temperature begins to raise *(see Fig. 7).* According to our experimental results, the regeneration starts earlier for a trap loaded with EUDC soot: the soot ignition temperature appeared to be around 450°C for EUDC soot, and around 490°C for ECE soot. Furthermore, as expected, a filter loaded with successive layers of EUDC and ECE soot starts to regenerate at the EUDC soot ignition temperature.

Even though the ignition temperature was always found to be the same for each type of soot, the propagation process of the regeneration through the DPF was a little random, yielding rather scattered results (as shown further on *Fig. 11*). This could be due to the difficulty to accurately control the many operating conditions on an engine test bench, or to the tendency of the soot to be swept away by the gas flow (*see next section*), and maybe also to the intrinsic nature of the soot.

2.3 Fuel-Borne Catalyst

Two additive contents were tested: 25 and 50 ppm. Our experimental results did not show much differences between those two values, with regard to the regeneration duration

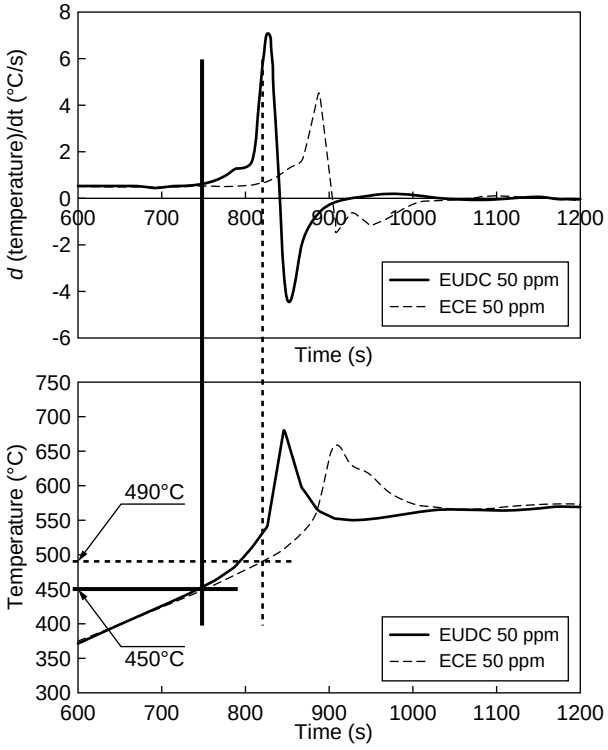

Figure 7

Determination of soot ignition temperature.

and the exothermicity. They both allowed the soot ignition temperature to drop from 550°C (no additive) down to about 470°C. The pressure drop still decreased a little for ECE soot between 25 and 50 ppm, as shown on Figure 8.

This pressure effect could not be observed on EUDC soot because it tended to be swept away towards the end of the filter, and prevented us to do any comparison. This tendency to pack may be related to the SOF (soluble organic fraction) of the soot: because the EUDC deposit layer contains less SOF than the ECE (0.2 instead of 9%, according to our analysis), it looks much dryer and more crumbly and is obviously more easily swept away by the gas flow.

3 DPF REGENERATION MODEL

Concurrently to this experimental study of the fuel-borne catalyst effect on the DPF regeneration, a 1D model was developed. It simulates the DPF regeneration, given the inlet gas flow and particulate loading characteristics, and is inspired by Bissett's work [4]. It describes what happens along an "inlet channel + deposit layer + substrate + outlet channel" set (*see Fig. 9*). The axial distance along the channel is called *z*. All variables in the inlet and outlet

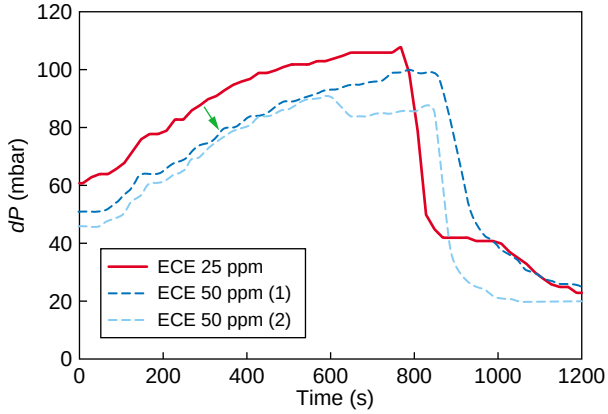

Figure 8

Effect of additive content on pressure drop (1 mbar = 100 Pa).

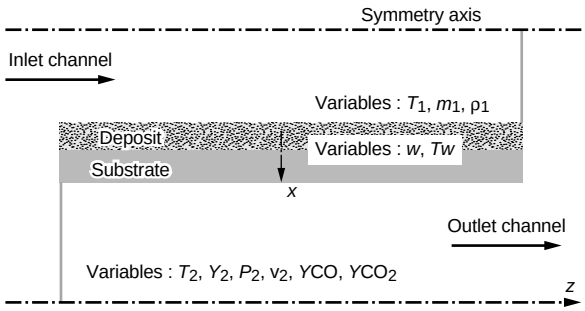

Figure 9

Domain simulated by the model.

channels only depend on z and on time t. In the porous medium, they also depend on x, distance through the deposit and the substrate.

3.1 Assumptions

We begin by assuming that the DPF behaves in a homogeneous way: all inlet channels may be represented by the behavior of a single channel, and the same holds for the outlet channels. This assumption will be discussed at the end of this paper.

The quantities T_i, ρ_i, v_i, etc. (i = 1, 2, w, for inlet, outlet channel, and wall) refer to quantities averaged over a channel or wall cross section. The gas flow can be divided into two components: a z-part flowing through the channel at the velocity v_i, and a perpendicular x-component flowing through the porous medium. As it is very thin, we assume that the flow rate Φ_w across the deposit layer and substrate is stationary:

$$\Phi_w = \text{cst} \tag{1}$$

The gas is assumed ideal, so the equation of state is:

$$P_i = r\rho_i T_i \tag{2}$$

We assume that T_w is the temperature of both phases in the porous medium and is independent of x, even though the heat from reaction is only produced in the deposit layer. Radiation heat transfer is neglected.

3.2 Inlet Channel

Conservation of mass

$$\frac{\partial \rho_1}{\partial t} + \frac{\partial(\rho_1 v_1)}{\partial z} = -\frac{4\Phi_w}{(D-2w)^2} \tag{3}$$

We take into account the gas that flows through the porous walls, and also the fact that the channel is partly obstructed by the deposit layer thickness w.

Navier-Stockes's equation

$$\frac{\partial(\rho_1 v_1)}{\partial t} + \frac{\partial(\rho_1 v_1^2)}{\partial z} + \frac{\partial P_1}{\partial z} = -\frac{a}{(D-2w)^2}\mu(T_1)v_1 \tag{4}$$

Since the gas is assumed to flow perpendicularly to the channel walls as it leaves the channel, there is no z-component of momentum through the wall to be transported, as in (3). A viscous drag is produced at the wall, to reduce the z-velocity to zero, which is represented by the right hand side (r.h.s.) of (4) (as suggested by [4]). The a coefficient value is specific of a fully developed laminar flow in a square channel [7].

Energy balance in channel gas

$$\frac{\partial(\rho_1 c_p T_1)}{\partial t} + \frac{\partial(\rho_1 v_1 c_p T_1)}{\partial z} = -\frac{4\Phi_w}{(D-2w)^2} c_p T_w + 4h_1 \frac{T_w - T_1}{D-2w} \tag{5}$$

Conduction in the z-direction is expected to be negligible relative to the convective transport. The contribution of heat transfer between the gas flowing in the channel and in the wall is handled using the heat transfer coefficient h_1.

Conservation of oxygen

The depletion of oxygen in the reactive deposit layer does not influence the oxygen concentration in the inlet channel. $Y_1(z,t)$ remains constant.

3.3 Deposit Layer + Substrate + Gas

Darcy's law

The pressure drop across the porous medium is assumed to follow Darcy's law:

$$\frac{\partial P}{\partial x} = -\frac{\mu}{k_i} v_w \tag{6}$$

with $i = p$ (particulate) or s (substrate).

The particulate and substrate permeabilities for a SiC trap were studied by [8]. Equation (6) could be integrated, using equation (1), to give:

$$P_1^{\,2} - P_2^{\,2} = \mu(T_w) R T_w \Phi_w \left(\frac{1}{k_p} \ln \frac{D}{D-2w} + \frac{2 w_s}{k_s D} \right) \tag{7}$$

Carbon oxidation, oxygen consumption and CO/CO_2 emissions

All these quantities depend on the reaction mechanism and the kinetics that were chosen. The way there were calculated will be explained later in this paper *(section Kinetics).*

Although the model allows reaction throughout the deposit layer, we assumed that the reaction consumes the deposit by shrinking its thickness w, without changing its internal structure.

Energy balance in the wall

$$\begin{aligned} &\frac{\partial}{\partial t}\left(\rho_p c_{pp} w(D-w) T_w + \rho_s c_{ps} w_s (D + \frac{1}{2} w_s) T_w \right) = \\ &\frac{\Delta H}{M_c} \rho_p (D-2w) \frac{\partial w}{\partial t} \\ &-h_1 (D-2w)(T_w - T_1) - h_2 D (T_w - T_2) \\ &+ \frac{\partial}{\partial z}\left(\lambda_p w(D-w) + \lambda_s w_s (D + \frac{1}{2} w_s) \right) \frac{\partial T_w}{\partial z} \end{aligned} \tag{8}$$

The gas energy is neglected in the l.h.s. In the r.h.s., there are terms for both conductive and convective heat transport, as well as the heat produced by reaction.

3.4 Outlet Channel

The equations are the same as in the inlet channel, except that the outlet channel is free of particles, and that the gas composition varies along the trap during regeneration. Y_s (Yco_{2s}, Yco_s) is the oxygen (CO_2, CO) mass fraction in the gas flowing through the substrate, and ready to enter and to mix with the outlet channel flow.

Conservation of mass

$$\frac{\partial \rho_2}{\partial t} + \frac{\partial (\rho_2 v_2)}{\partial z} = 4 \frac{\Phi_w}{D^2} \tag{9}$$

Conservation of oxygen

$$\frac{\partial Y_2}{\partial t} + v_2 \frac{\partial (Y_2)}{\partial z} = 4 \frac{\Phi_w}{D^2} \left(\frac{Y_s - Y_2}{\rho_2} \right) \tag{10}$$

CO_2 and CO balances

$$\frac{\partial Y_{CO_{2_2}}}{\partial t} + v_2 \frac{\partial (Y_{CO_{2_2}})}{\partial z} = 4 \frac{\Phi_w}{D^2} \left(\frac{Y_{CO_{2S}} - Y_{CO_{2_2}}}{\rho_2} \right) \tag{11}$$

$$\frac{\partial Y_{CO_2}}{\partial t} + v_2 \frac{\partial (Y_{CO_2})}{\partial z} = 4 \frac{\Phi_w}{D^2} \left(\frac{Y_{CO_s} - Y_{CO_2}}{\rho_2} \right) \tag{12}$$

Navier-Stokes's equation

$$\frac{\partial (\rho_2 v_2)}{\partial t} + \frac{\partial P_2}{\partial z} + \frac{\partial (\rho_2 v_2^{\,2})}{\partial z} = -a \mu(T_2) \frac{v_2}{D^2} \tag{13}$$

Energy balance

$$\begin{aligned} &\frac{\partial (\rho_2 c_p T_2)}{\partial t} + \frac{\partial (\rho_2 v_2 c_p T_2)}{\partial z} = \\ &\qquad 4 \frac{\Phi_w}{D^2} c_p T_w + 4 \frac{h_2}{D} (T_w - T_2) \end{aligned} \tag{14}$$

These equations are associated to the appropriate boundary and initial conditions: the temperature and the flow rate at the inlet of the DPF are known and can vary with time. The flow rate is zero at both plugged channel ends (inlet and outlet). The outlet pressure is taken to be atmospheric. Any local heat loss from the solid phase at the front or rear faces are neglected. The initial deposit layer thickness can vary along the inlet channel, and so be either homogeneous or packed in the trap bottom.

4 KINETICS

The kinetic constants used in our DPF model were experimentally determined by running a fixed bed reactor under isothermal conditions. The experiments were like those described precisely by [9, 10]: a 10 mg sample of soot was heated to the reaction temperature under inert gas (N_2). At time zero, the gas flow was then switched to an O_2-N_2 mixture. A flow rate of 100 l/h was used. CO and CO_2 concentrations were recorded during the whole soot oxidation process, and used to calculate the reaction rates. The soot sample was mixed with quartz beads so as to limit temperature rises due to the exothermic reaction of soot (less than 3 K) and hence to ensure a slow reaction, and make sure that the O_2 gradient that develops across the sample remains negligible.

We describe in this section the kind of reaction mechanism we used, how we determined all kinetic constants

from our fixed bed reactor experimental results, and the way we integrated them in the DPF model.

Although much research has been performed on non-additivated and additivated soot oxidation, the detailed kinetics of soot oxidation have hardly been studied. We used five global reactions to describe the additivated soot oxidation:

– Direct oxidation of carbon with oxygen:

$$(-C) + O_2 \xrightarrow{k_1} CO_2 \qquad (r_1)$$

$$2(-C) + O_2 \xrightarrow{k_2} CO \qquad (r_2)$$

– Carbon oxidation with metallic oxide:

$$(-C) + 2(-MO) \xrightarrow{k_{11}} CO_2 + 2(-M-) \qquad (r_3)$$

$$(-C) + (-MO) \xrightarrow{k_{12}} CO + (-M-) \qquad (r_4)$$

– Re-oxidation of reduced metallic sites with molecular oxygen:

$$2(-M-) + O_2 \xrightarrow{k_3} 2(-MO) \qquad (r_5)$$

The additive allows the carbon (–C) to be oxidized by switching between its own most oxidized form (–MO) and its reduced form (–M). This mechanism has been suggested by several authors [11, 12].

Given this reaction mechanism, we can write the expression of the consumption rate of the metallic oxide and of the carbon contained in the deposit layer, assuming that these global reactions follow Arrhenius' laws:

$$\frac{d\varepsilon}{dt} = -\delta(1-\zeta)\left(k_{11}\varepsilon^2 + k_{12}\varepsilon\right) + k_3(1-\varepsilon)^2 P_{O_2} \qquad (15)$$

$$\frac{d\zeta}{dt} = \delta(1-\zeta)\left(k_{11}\varepsilon^2 + k_{12}\varepsilon\right) + (1-\delta)\left[k_1 {m_0}^{\beta_1 - 1}(1-\zeta)^{\beta_1} + k_2 {m_0}^{\beta_2 - 1}(1-\zeta)^{\beta_2}\right] P_{O_2}^{\alpha} \qquad (16)$$

where ε is the proportion of oxidized metallic sites, and δ is the additive content in soot. ζ is the carbon consumption rate, defined as:

$$\zeta = 1 - \frac{m(t)}{m_0} \qquad (17)$$

where m_0 is the initial mass of carbon, present in the reactor, and *m(t)* is its value as a function of time.

4.1 Non-Additivated Soot

We began by studying the kinetics of non-additivated soot, to determine k_1, k_2, α, β_1, and β_2. In this case, δ = 0, so only the Reactions (r_1) and (r_2) remain, and Equation (16) simplifies to:

$$\frac{d\zeta}{dt} = \left[k_1 {m_0}^{\beta_1 - 1}(1-\zeta)^{\beta_1} + k_2 {m_0}^{\beta_2 - 1}(1-\zeta)^{\beta_2}\right] P_{O_2}^{\alpha} \qquad (18)$$

where k_i follows an Arrhenius's law:

$$k_i = K_i \exp\left(-E_i / RT\right)$$

The reaction orders in carbon, β_i, were determined by fitting the experimental combustion curves, following the expression, deduced from (18) for a given temperature and O_2 concentration:

$$\log\left(\frac{d\zeta}{dt}\right) = \beta_i \log(1-\zeta) + \text{cst}$$

for both CO and CO_2.

In this same approach, the reaction order in oxygen was studied for a given temperature and carbon consumption rate, in the range 5-15% O_2, which is typical of Diesel exhaust gas concentration. And the activation energy was determined by running the reactor for different temperatures between 450 and 700°C, at a given carbon consumption rate and O_2 concentration. α and β_i were found to be around 0.6, and E_i equal to 190 000 J/mol. This last value is of the same order of magnitude magnitude as those found by [6, 10, 13], and others.

4.2 Additivated Soot

Additivated soot starts to oxidize at a much lower temperature than non-additivated soot, as Reactions (r_3) to (r_5) are more reactive. Those reactions kinetics were studied on a fixed bed reactor as well. It was run isothermally for temperatures ranging from 390 to 450°C, in order to determine k_{11}, k_{12} and k_3. k_3 was found to be very large, so that the re-oxidation Reaction (r_5) was very fast, and that any reduced additive was re-oxidized at once. Therefore, ε could be taken equal to 1.

4.3 Integration in DPF Model

Once we know the kinetic constants, we can use them to calculate the O_2, CO_2 and CO gradients through the deposit layer.

All "*s*" quantities were analytically resolved, as they vary in the *x*-direction. The eleven quantities varying in the

z-direction form a system of nonlinear partial differential equations, of the form:

$$\frac{\partial U}{\partial t} = f\left(t, U, \frac{\partial U}{\partial z}, \frac{\partial^2 U}{\partial z^2}\right)$$

This system was solved by using a package of Fortran' subroutines designed to solve such a system [14].

5 MODEL VALIDATION AND DISCUSSION

5.1 Inlet Data and Initial Soot Mass

Some data are directly taken from the engine tests and used in the model. It concerns the gas flow rate entering the DPF, oxygen, CO and CO_2 contents, and temperature. All these parameters can vary with time. The loaded soot mass is used to calculate the initial deposit layer thickness. It is also important to make it clear here that the pressure drop depends on the total soot amount remaining in the trap, while the oxidation only concerns the carbon quantity, which is about 80% of the soot mass. The Figure 10 shows how much it is important to use the right mass for each of those modeled quantities: if we only use the total mass, the pressure drop is well simulated but not the peak temperature, and vice versa if we only use 80% of the total mass.

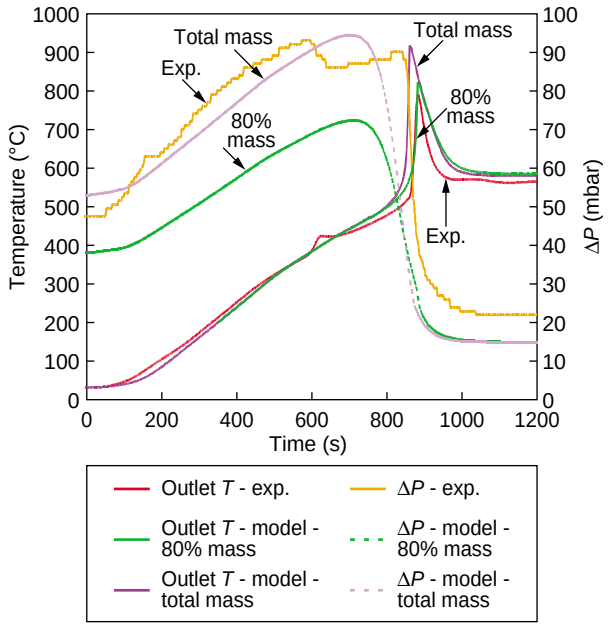

Figure 10

Model: influence of the soot mass on pressure drop and heat of reaction.

5.2 ECE and EUDC

As can be seen on Figure 10, our model yields results in good agreement with the experiment. The kinetics constants used for ECE and EUDC soot are gathered in Table 1. The additive content effect was taking into account through the value of δ.

The numerical results obtained with our model are presented on Figure 11, together with our experimental results, for 50 ppm ECE and EUDC soot, and various engine operating conditions. Each graph only shows the moment when the regeneration and its peak temperature occur. Given the scattering of our experimental results, the agreement between the model and the real DPF is pretty good. The location of the peak temperature is well predicted.

TABLE 1

Kinetic constants used in the regeneration model

25 and 50 ppm	ECE	EUDC
K_1	$3\ 10^4$	$4\ 10^4$
K_2	$7\ 10^4$	$6\ 10^4$
K_{11}	$8.4\ 10^8$	$9.8\ 10^8$
K_{12}	$2.4\ 10^8$	$2.8\ 10^8$
E_1 and E_2 (kJ/mol)	190	190
E_{11} and E_{12} (kJ/mol)	160	60

However, the simulated exothermicity starts about 100 s too early, *i.e.* around 400°C, and more slowly than in the experiment. It also takes a longer time to decrease. Two reasons can be put forward:

– Our main assumption, which allows our model to be one-dimensional, is that all inlet channels behave the same way, so that inlet conditions are homogeneous for them all, and heat losses upstream and along the filter are neglected. This is far from reality, as we actually observe a radial temperature gradient that is already about 40°C upstream the filter and can reach 80°C inside the DPF. That is why we observe that the channels around the DPF axis regenerate faster than those near its periphery, as shown on Figure 12. In addition, the flow rate per channel is strongly coupled to the regeneration rates of all channels. All these comments highlight the need for a multi-dimensional model, that would predict more accurately the temperature variations in the DPF.

– The way the regeneration progresses in the channel is also directly related to the kinetics. It would be useful to study them more closely, to explain how the soot reaction heat is released in such a short time. We may have to choose new kinetic constants, such as higher activation energies, or even to develop a more precise reaction mechanism.

a) 50 ppm catalyzed soot experiments - 10% O_2 and 75 kg/h

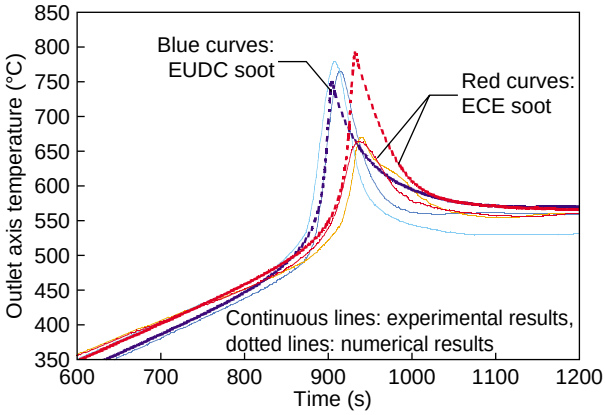

b) 50 ppm catalyzed soot experiments - 15% O_2 and 85 kg/h

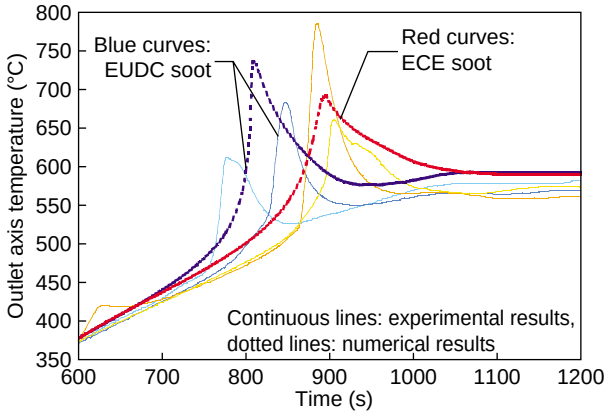

c) 50 ppm catalyzed soot experiments - 10% O_2 and 140 kg/h

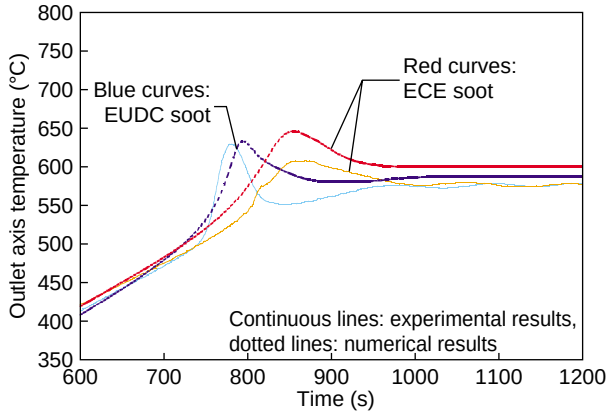

Figure 11

Comparison between experimental and numerical results, for various operating conditions.

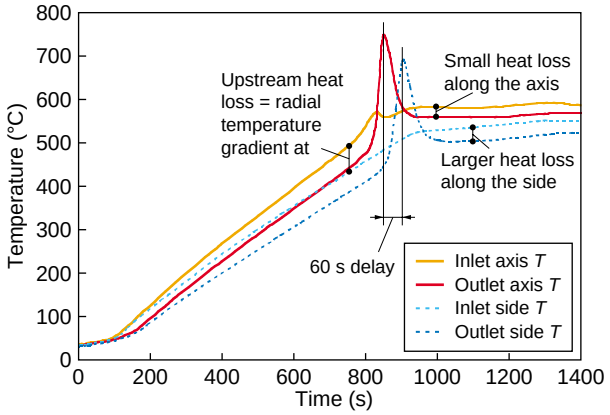

Figure 12

Experimental temperature radial variations in the DPF regeneration.

5.3 Influence of Soot Packing

According to our experiments, and as shown on Figure 13, the exothermicity is higher when the soot has been swept away towards the end of the inlet channel than when the deposit layer remains homogeneous. That was expected, since the local reaction heat release is directly related to the higher amount of soot available. The numerical results obtained for an example of packed deposit layer are presented on Figure 14, together with those obtained for a homogeneous layer. It appears that our model is also able to predict such a higher peak temperature.

CONCLUSIONS

The experimental part of this work, run on an engine test bench, highlights the way the fuel-borne catalyst diminishes the soot ignition temperature, and assists the DPF regeneration. The kinetics were determined separately on a fixed bed reactor. A 1D model is described, which simulates the regeneration progress along an “inlet channel + deposit layer + substrate + outlet channel” set, and integrates the additive action. The numerical and experimental results are in good agreement.

Both experimental and numerical works allow us to better understand the additive action on DPF regeneration:

– The soot ignition temperature drops from 550°C without additive down to 450°C for EUDC soot and 490°C for ECE soot. We did not notice any significant difference between the two additive contents that were studied (25 and 50 ppm). And if the loading is composed of different types of soot, the lower soot ignition temperature prevails

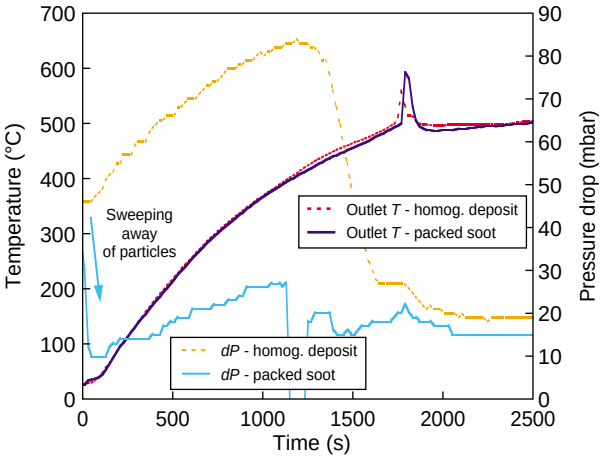

Figure 13

Soot packing – experimental results.

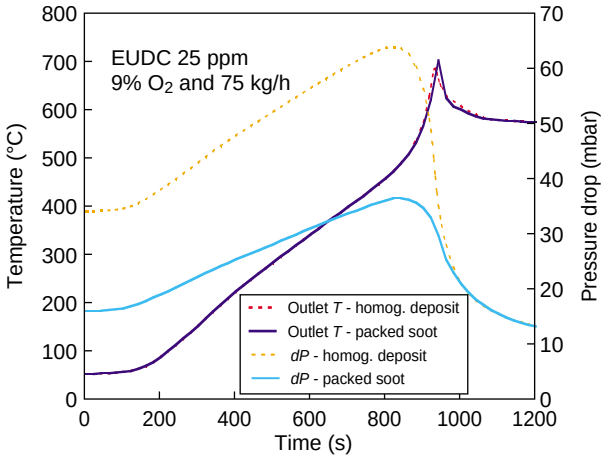

Figure 14

Soot packing – model prediction.

for the whole.

– Both experimental and numerical studies show that the exhaust flow rate entering the monolith has a dominant effect on the regeneration progress, and that the oxygen content does not, but it was only investigated for 10 and 15%, which are both rather high values.
– The additivated soot tends to be swept away during regeneration, especially for soot with a very small soluble organic fraction, such as EUDC. The soot packed to the end of the inlet channel creates then a higher peak temperature. The model is also able to predict this additional heat release.

As we suggest in this paper, there are two possibilities of development to further improve our understanding of the DPF regeneration, and the agreement between the experimental results and the model predictions. The first one is to develop a multi-channel model, in order to take into account the non homogeneous distribution of temperature and gas flow rate that we actually observe at the filter inlet, and the heat exchanges between the axis and the periphery inside the filter. The other possibility of improvement is to further study the details of the soot reaction kinetics. Such investigations will be presented in a next paper.

ACKNOWLEDGEMENTS

We would like to thank J.F. Brilhac, P. Gilot and the *LGRE (Laboratoire de gestion des risques et de l'environnement)* at the *Université de Haute-Alsace* for investigating the soot kinetics, F. Kerdelhue who took care of the engine test bench experimental part, and the *ADEME* (French agency for energy and environment) for its financial support.

REFERENCES

1 Gishoff, J., Pfeifer, M., Schäfer-Sindlinger, A., Hackbarh, U., Teysset, O., Colignon, C., Rigaudeau, C., Salvat, O., Krieg, H. and Wenclawiak, B.W. (2001) Regeneration of Catalytic Diesel Particulate Filters. *SAE Paper 2001-01-0907.*

2 Hoffmann, U., Rieckmann, T. and Ma, J. (1991) Kinetic Study and Modelling of Diesel Particulate Filter Regeneration. *Chem. Eng. Science*, **46,** 4, 1101-1113.

3 Koltsakis, G.C. and Stamatelos, A.M. (1996) Modeling Catalytic Regeneration of Wall-Flow Particulate Filter. *Ind. Eng. Chem. Res.*, 35, 2-13.

4 Bissett, E.J. (1984) Mathematical Model of the Thermal Regeneration of a Wall-Flow Monolith Diesel Particulate Filter. *Chem. Eng. Sc.*, **39,** 7/8, 1233-1244.

5 Konstandopoulos, A.G., Kostoglou, M. and Housiada, P. (2001) Spatial Non-Uniformities in Diesel Particulate Trap Regeneration. *SAE Paper 20001-01-0908.*

6 Bissett, E.J. and Shadman, F. (1985) Thermal Regeneration of Diesel-Particulate Monolithic Filters. *AiChe Journal*, **31,** 5, 753-758.

7 Shah, R.K. and London, A.L. (1978) *Laminar Flow in Forced Convection Ducts*, Academic Press, 196-205.

8 Versaevel, P., Colas, H., Rigaudeau, C., Noirot, R., Koltsakis, G.C. and Stamatelos, A.M. (2000) Some Empirical Observations on Diesel Particulate Filter Modeling and Comparison Between Simulations and Experiments. *SAE Paper 2000-01-0477.*

9 Stanmore, B.R., Brilhac, J.F. and Gilot, P.(1999) The Ignition and Combustion of Cerium Doped Diesel Soot. *SAE Paper 1999-01-0115.*

10 Neeft, J.P.A., Nijhuis, T.X., Smakman, E., Makkee, M. and Moulijn, J.A. (1997) Kinetics of the Oxidation of Diesel Soot. *Fuel*, **76,** 12, 1129-1136.

11 De Soete, G. (1988) Catalysis of Soot Combustion by Metal Oxides'. In *Western States Section Meeting, The Combustion Institute*, Salt Lake City, 21-22 March.

12 Neeft, J.P.A. (1995) Catalytic Oxidation of Soot: Potential for the Reduction of Diesel Particulate Emissions. *Thesis*, Delft, Netherlands, ISBN 902-9008768-0.

13 Koltsakis, G.C. and Stamatelos, A.M. (1996) Modeling Thermal Regeneration of Wall-Flow Diesel Particulate Trap. *AiChe Journal*, **42,** 6, 1662-1672.

14 Sincovec, R.F. and Madsen, N.K. (1975) Software for Nonlinear Partial Differential Equations.*Transactions on Mathematical Software*, **1**, 3, 232-260.

Final manuscript received in November 2002